HHS Public Access

Author manuscript

Nat Med. Author manuscript; available in PMC 2012 March 01.

Published in final edited form as:

Nat Med. ; 17(9): 1094–1100. doi:10.1038/nm.2438.

Imatinib potentiates anti-tumor T cell responses in gastrointestinal stromal tumor through the inhibition of Ido

Vinod P. Balachandran[1], **Michael J. Cavnar**[1], **Shan Zeng**[1], **Zubin M. Bamboat**[1], **Lee M. Ocuin**[1], **Hebroon Obaid**[1], **Eric C. Sorenson**[1], **Rachel Popow**[1], **Charlotte Ariyan**[1], **Ferdinand Rossi**[2], **Peter Besmer**[2], **Tianhua Guo**[3], **Cristina R. Antonescu**[3], **Takahiro Taguchi**[4], **Jianda Yuan**[5], **Jedd D. Wolchok**[5,6], **James P. Allison**[5,7], and **Ronald P. DeMatteo**[1]

[1]Department of Surgery, Memorial Hospital, New York

[2]Developmental Biology, Sloan-Kettering Institute, New York

[3]Department of Pathology, Memorial Hospital, New York

[4]Division of Human Health and Medical Science, Graduate School of Kuroshio Science, Kochi University, Japan

[5]The Ludwig Center for Cancer Immunotherapy, New York

[6]Department of Medicine, Memorial Hospital, New York

[7]Immunology Programs, Sloan-Kettering Institute, New York

Abstract

Imatinib mesylate targets mutated KIT oncoproteins in gastrointestinal stromal tumor (GIST) and achieves a clinical response in 80% of patients. The mechanism is believed to depend predominantly on the inhibition of KIT-driven signals for tumor cell survival and proliferation. Using a mouse model of spontaneous GIST, we found that the immune system contributes substantially to the anti-tumor effects of imatinib. Imatinib therapy activated $CD8^+$ T cells and induced regulatory T cell (T reg) apoptosis within the tumor by reducing tumor cell expression of the immunosuppressive enzyme indoleamine 2,3-dioxygenase (Ido). Concurrent immunotherapy augmented the efficacy of imatinib in mouse GIST. In freshly obtained human GIST specimens, the T cell profile correlated with imatinib sensitivity and IDO expression. Thus, T cells are critical

Correspondence: Ronald P. DeMatteo, Memorial Sloan-Kettering Cancer Center, 1275 York Avenue, New York, NY 10065, Tel: (212) 639-3976, Fax: (212) 639-4031, dematter@mskcc.org.

AUTHOR CONTRIBUTIONS

All authors contributed to experimental design. V.P.B., M.J.C., S.Z., Z.B., H.O., R.P., C.A., T.G., C.R.A., and J.Y. performed the experiments. All authors assisted in data analysis. V.P.B. and R.P.D. wrote and prepared the manuscript with critical comments from all authors.

COMPETING FINANCIAL INTERESTS

Ronald P. DeMatteo serves as a consultant for Novartis and has received honoraria. Peter Besmer has received a commercial research grant from Novartis. Jedd D. Wolchok serves as a consultant to Novartis and Bristol-Meyers Squibb. CTLA-4 blocking antibody is currently in clinical development by Medarex and Bristol-Meyers Squibb. James P. Allison is a consultant for Medarex and Bristol-Meyers Squibb and is an inventor of intellectual property that has been licensed to Medarex and Bristol-Meyers Squibb by the University of California-Berkeley.

to the anti-tumor effects of imatinib in GIST and concomitant immunotherapy may further improve outcome in human cancers treated with targeted agents.

Keywords

Imatinib mesylate; gastrointestinal stromal tumor; Ido; T cells

INTRODUCTION

GIST originates in the gastrointestinal tract and is the most common gastrointestinal sarcoma.[1] Approximately 75–80% of GISTs contain an activating *KIT* mutation, while 5–10% instead have a platelet-growth factor receptor alpha (*PDGFRA*) mutation.[2,3] Imatinib mesylate is a small molecule inhibitor of KIT, PDGFRA, ABL, and BCR-ABL tyrosine kinases. Imatinib induces a clinical response in approximately 80% of patients with advanced GIST and improves median overall survival from 9 months to over 5 years.[4,5] Imatinib therapy for GIST is one of the most successful applications of targeted molecular therapy and has prompted the development of novel targeted agents for a variety of other cancers.

Despite its effectiveness, imatinib is almost never curative in GIST. Disease progression occurs at a median of 18 months, most often due to the emergence of resistant clones with secondary *KIT* or *PDGFRA* mutations.[1] One potential strategy to increase the efficacy of imatinib is to combine it with immunotherapy. Currently, our understanding of the immune response to GIST is limited. Immunohistochemistry in human GIST demonstrated the presence of intratumoral $CD8^+$ T cells, T regs, and macrophages.[6,7] In GIST patients who were treated with imatinib, progression-free survival correlated with IFN-γ secretion by peripheral blood natural killer (NK) cells.[8] Imatinib has also been shown to induce dendritic cells to activate NK cells in mice with other tumors,[9] although NK cells were largely absent in human GIST specimens.[7] Overall, then, the importance of the immune system in GIST patients treated with imatinib remains largely undefined. Therefore, we studied the immune response to GIST during imatinib therapy to assess the potential of combining targeted and immune therapy.

RESULTS

$CD8^+$ T cells contribute to anti-tumor effects of imatinib

To investigate the role of the immune response to imatinib in GIST, we utilized a transgenic mouse ($Kit^{V558\Delta/+}$) that spontaneously develops a single GIST in the cecum by 4 weeks of age due to an activating mutation in the *Kit* gene.[10] The tumor is similar to human GIST in morphology, oncogenic Kit signaling, and sensitivity to imatinib (Supplementary Fig. 1).[10,11] Imatinib rapidly decreased tumor weight (Fig. 1a, Supplementary Fig. 1), which correlated with a specific loss of Kit^+ tumor cells (Supplementary Fig. 1). By day 8, tumors had less uptake of ^{18}fluoro-deoxyglucose (FDG) by positron emission tomography (PET) scans (Fig. 1b), as occurs in humans.[1] Imatinib increased the number and activation of $CD8^+$ T cells in the mesenteric draining lymph nodes (DLNs) of GIST mice but not the inguinal

nodes of GIST mice or DLNs of WT mice (Fig. 1c). Imatinib increased the frequency of tumor-specific $CD8^+$ T cells in the DLN (Fig. 1d). Within the tumor, imatinib induced a dramatic increase in $CD8^+$ T cell frequency, number (Fig. 1e), and proliferation (Fig. 1f). Activation measured by CD69 expression and cytolytic capacity determined by granzyme B expression were also increased (Fig. 1g). Histology revealed that $CD4^+$ (data not shown) and $CD8^+$ T cells diffusely infiltrated the tumor at baseline (Fig. 1h). After imatinib, there was no change in the production of IL-4, IL-17, or IFN-γ by $CD4^+$ T cells (Supplementary Fig. 2) or in the frequency of myeloid cells, B cells, NK, or NKT cells (Supplementary Fig. 3).

To identify the importance of $CD8^+$ T cells during imatinib therapy, we depleted them with a monoclonal antibody. The anti-tumor effects of imatinib were blunted in mice depleted of $CD8^+$ but not $CD4^+$ T cells, NK cells (Fig. 1i), or myeloid cells (Supplementary Fig. 4). GIST-$RAG1^{-/-}$ mice had larger tumors than aged-matched controls but GIST-μMT^- mice lacking B cells did not (Supplementary Fig. 4). Furthermore, imatinib naïve GIST mice depleted of $CD8^+$ but not $CD4^+$ T cells, NK cells, or B cells had larger tumors (Supplementary Fig. 4). Taken together, imatinib amplifies a pre-existing immune response in mouse GIST and $CD8^+$ T cells are required for its maximal effects.

Imatinib modulates intratumoral T cells through inhibition of Ido

We next analyzed whether imatinib altered T regs, since they play a vital role in the suppression of anti-tumor immune responses.[12] Remarkably, imatinib decreased the frequency and number of T regs in the tumor, but not in the DLN (Fig. 2a) or spleen (data not shown). Consistent with this finding, T reg apoptosis occurred selectively within the tumor (Fig. 2b). As a result, imatinib significantly increased the intratumoral $CD8^+$ T cell to T reg ratio within the tumor, but not in the DLN (Fig. 2c) or spleen (data not shown). The intratumoral T effector to T reg ratio is known to correlate with a favorable immunological outcome against tumors in both mice and humans.[13–15]

To identify how imatinib affected intratumoral $CD8^+$ T cells and T regs, we performed gene expression array analysis of mouse GIST tumors. Among the largest differences after imatinib was a reduction in intratumoral *Ido* mRNA (Supplementary Table 1; Fig. 3a, **left panel**). Immunomodulatory cytokines IL-1β, IL-6, TNF-α, IL-17, IL-10, and IFN-γ were not altered by imatinib (Supplementary Fig. 5). Ido is a protein that catalyzes the conversion of tryptophan into immunosuppressive metabolites, which promote the development, stabilization, and activation of T regs while also suppressing effector T cells.[16–21] Western blot confirmed that Ido protein was expressed at high levels at baseline within the tumor but not in the DLN or spleen, and was decreased substantially by imatinib (Fig. 3a, **center**). Ido protein was present in $CD45^-$ Kit^+ tumor cells but not $CD45^+$ intratumoral lymphocytes (Fig. 3a, **right**). The overall reduction in tumor Ido protein by imatinib did not result merely from the loss of tumor cells, since Ido protein was also decreased on a per cell basis in live tumor cells (Fig. 3a, **right**).

To determine whether the reduction of intratumoral Ido levels had functional consequences, we administered the specific Ido inhibitor 1-methyl-D-tryptophan (1-MT) to GIST mice. 1-MT alone decreased tumor weight, and notably $CD8^+$ T cells were required for this effect (Fig. 3b). Ido blockade alone increased the proliferation and activation of intratumoral $CD8^+$

T cells (Fig. 3c), but not other immune cells (data not shown). Furthermore, the number and frequency of intratumoral T regs were reduced (data not shown) due to T reg apoptosis within the tumor but not in the DLN (Fig. 3d). Apoptosis occurred preferentially in T regs and was not observed in $CD8^+$ T cells or other immune cells with Ido inhibition (data not shown). As a result, there was an increase in the intratumoral $CD8^+$ T cell to T reg ratio (Fig. 3e).

These observations from Ido inhibition were reminiscent of our findings in GIST mice treated with imatinib. So we hypothesized that the immune effects of imatinib are partially mediated by its reduction of Ido. To test this, we treated GIST mice with imatinib and a cocktail of immunosuppressive tryptophan metabolites (L-kynurenine, 3-hydroxyanthranilic acid, and 3-hydroxykynurenine) to circumvent Ido inhibition during imatinib therapy. The administration of tryptophan metabolites diminished the anti-tumor effects of imatinib (Fig. 3f). Of note, concomitant administration of 1-MT did not increase the anti-tumor effects of imatinib, consistent with their potential overlapping mechanisms (Fig. 3f). Tryptophan metabolites effectively blocked imatinib-mediated upregulation of CD69 and granzyme B in intratumoral $CD8^+$ T cells (Fig. 3g) and apoptosis of intratumoral T regs (Fig. 3h), thereby preserving the baseline intratumoral $CD8^+$ T effector to T reg ratio (Fig. 3i). Thus, our data suggest that imatinib induces intratumoral $CD8^+$ T cell activation and regulatory T cell apoptosis in mouse GIST through the inhibition of Ido.

Imatinib reduces IDO by inhibiting oncogenic KIT signaling

To establish how imatinib reduced tumor cell expression of Ido, we analyzed a human GIST cell line (GIST-T1) in which oncogenic KIT signaling is driven by a *KIT* exon 11 mutation,[22] similar to our mouse model. We also performed additional studies using a subclone of GIST-T1 called GIST-T1R, which became resistant to imatinib after chronic, intermittent exposure to the drug during culture. GIST-T1R cells acquired a secondary mutation in *KIT* exon 13, V654A, as can occur in human GIST patients.[23] Imatinib potently inhibited IDO expression in live GIST-T1 cells on a per cell basis but not in GIST-T1R cells, suggesting that imatinib-mediated reduction of IDO depended on its ability to block KIT signaling (Fig. 4a). Imatinib rapidly decreased *Ido* mRNA at 6 and 12 h *in vivo* in bulk tumor and sorted tumor cells (Fig. 4b). IFN-α, IFN-β, and IFN-γ are among the strongest inducers of IDO.[24] IFN-α and IFN-β signaling depend on the translational repressor 4-EBP1 and transcriptional activator S6, both of which are activated by mammalian target of rapamycin (mTOR).[25–28] mTOR is a downstream component of the oncogenic KIT-PI3K-AKT pathway that is constitutively active, central to GIST oncogenesis, and inhibited by imatinib.[11] Rapamycin, an inhibitor of mTOR, was sufficient to reduce IDO expression in GIST-T1 cells (Fig. 4c).

To identify other potential regulators of *Ido* transcription, we analyzed predicted binding sites within its promoter region (Genomatix, Munich, Germany). Etv4, a transcription factor and one of the genes with the greatest magnitude of reduction on our array (Supplementary Table 1, Fig. 4d), was identified as a highly likely candidate. Imatinib rapidly reduced *Etv4* mRNA *in vivo* in bulk tumor and sorted tumor cells (Fig. 4e). In addition, imatinib decreased IDO and ETV4 protein in mouse tumors and GIST-T1 cells and also reduced

phosphorylated KIT, STAT3, and S6 (Fig. 4f) as previously shown.[11] Consistent with the potential of Etv4 to regulate *Ido* transcription, Etv4 bound to the *Ido* promoter by chromatin immunoprecipitation (ChIP) in vehicle treated mice, but not in imatinib treated mice (Fig. 4g).

T cell profile correlates with imatinib sensitivity in human GIST

To determine the clinical relevance of our findings in mouse GIST, we analyzed the immune infiltrate in 45 matched blood and tumor specimens that were freshly obtained from 36 individuals with GIST undergoing surgery (Supplementary Table 2). Tumors were classified as sensitive or resistant to imatinib (based on serial radiologic assessment) or as untreated.

When compared with resistant tumors, sensitive tumors contained greater frequencies of $CD3^+$ and $CD8^+$ T cells, but a lower percentage of $CD4^+$ T cells (data not shown) and T regs (Fig. 5a). Immunohistochemistry confirmed the presence of $CD8^+$ and $CD4^+$ T cells and T regs infiltrating human GISTs (Supplementary Fig. 6, data not shown). There were no differences in intratumoral NK cells based on tumor response (Supplementary Fig. 6). Irrespective of treatment status and tumor response, intratumoral $CD8^+$ T cells were activated based on CD69 and CD25 expression when compared with $CD8^+$ T cells from the blood of the same patient (Fig. 5b). Consistent with our findings in mouse GIST, the intratumoral $CD8^+$ T cell to T reg ratio was increased in imatinib-sensitive tumors compared with untreated tumors (Fig. 5c). Notably, the intratumoral $CD8^+$ T cell to T reg ratio was lower in resistant tumors compared with sensitive GISTs (Fig. 5c). In 2 of 3 patients who had coexistent sensitive and resistant tumors removed simultaneously, we observed a higher $CD8^+$ T cell to T reg ratio in the sensitive tumors (Fig. 5d). Moreover, in 13 patients whose freshly isolated tumors were tested immediately for IDO by flow cytometry, the intratumoral $CD8^+$ T effector to T reg ratio correlated with IDO protein expression (Fig. 5e). IDO protein demonstrated a trend in distinguishing sensitive and resistant tumors with significantly higher *IDO* mRNA in resistant compared to sensitive tumors (Supplementary Fig. 7). Thus, the intratumoral T cell profile correlates to treatment response and IDO expression in human GIST.

Imatinib and CTLA-4 blockade are synergistic in mouse GIST

Although imatinib is highly effective, the drug eventually fails in the vast majority of GIST patients. Given our finding that imatinib therapy depends on $CD8^+$ T cells for its maximal effects, we investigated whether additional immune activation could augment its efficacy. We tested the combination of imatinib and blockade of cytotoxic T lymphocyte-associated antigen 4 (CTLA-4), a known modulator of effector T cells, T regs, and Ido.[29,30]

Concurrent administration of imatinib and induction treatment with CTLA-4 specific blocking antibody for 1 week followed by chronic CTLA-4 blockade significantly decreased tumor size in established mouse GISTs compared with either treatment alone (Fig. 6a, Supplementary Figure 8). It has been shown that CTLA-4 blockade during priming can lead to accumulation of $CD8^+$ T cells capable of producing effector cytokines such as IFN-γ.[31] GIST mice treated with imatinib and CTLA-4 blockade demonstrated no change in the frequency or absolute number of $CD4^+$ or $CD8^+$ T cells in DLN or tumor (Fig. 6b, c), or the

$CD8^+$ T effector to T reg ratio in the tumor (Fig. 6d). Intratumoral $CD8^+$ T cells demonstrated a trend of enhanced IFN-γ production (Fig. 6e). Therefore, combined therapy of imatinib and CTLA-4 blockade has potential therapeutic promise for human GIST and may exert anti-tumor effects by increasing IFN-γ producing $CD8^+$ T cells.

DISCUSSION

The discovery that oncogenic signaling pathways can be selectively inhibited using targeted agents has revolutionized the treatment of cancer.[32] While imatinib is thought to act primarily via direct effects on tumor cells, here we show that it also relies considerably on indirect effects from the immune system. It is noteworthy that we found $CD8^+$ T cell activation even though imatinib has been reported to block phosphorylation of $CD8^+$ T cell leukocyte-specific protein tyrosine kinase (LCK) *in vitro*,[33] although this may require supraphysiologic doses.[34] Our findings do not exclude the importance of other immune effectors during imatinib therapy, although depletion of $CD4^+$ T cells or NK cells did not affect tumor weight and the frequency of intratumoral NK cells did not correlate with treatment status in human GIST. While imatinib did not alter $CD8^+$ T cells in the DLN or spleen of WT mice, both direct effects of imatinib on immune cells and indirect effects such as through the release of tumor cell contents may be important in *Ido* transcription and T cell modulation. Further study will be necessary to identify the specific tumor antigens in mouse GIST. Human GISTs variably express cancer-testis antigens.[35] Nevertheless, identification of the immunoreactive epitopes for a particular GIST may be unnecessary, since imatinib may act as a vaccine through tumor destruction.

T regs are essential to tumor-induced peripheral tolerance and are a barrier to tumor immunotherapy.[12] Some cytotoxic agents deplete T regs systemically.[36] Previously, imatinib reduced spleen T regs in Balb/C mice, albeit only in the absence of tumor.[37] We did not find that imatinib altered T reg frequency in the spleen or DLN (Fig. 2a) of GIST mice or in the blood of patients (Fig. 5a). Therapeutic strategies to deplete T regs solely within the tumor are attractive to avoid inducing autoimmunity from global T reg depletion. Recently, stimulation of glucocorticoid-induced tumor necrosis factor receptor (GITR) alone or cyclophosphamide combined with OX40 stimulation was shown to deplete intratumoral T regs selectively in mouse melanoma, but the mechanism was not identified.[15,38] We found that imatinib selectively reduced intratumoral T regs by inhibiting Ido expression in GIST mice. Thus, while GIST cells exhibit “oncogene addiction” to *KIT*, intratumoral T regs in mouse GIST demonstrated “Ido addiction.”[39] Our findings support the notion that tumors create mutually reliant immunosuppressive networks. Ido is critical to T regs[17,19–21] and conversely, ligands expressed by T regs induce Ido.[16,40] IDO appears to be instrumental in human cancers,[41] and we found that the intratumoral $CD8^+$ T cell to T reg ratio correlated with intratumoral IDO expression in patients (Fig. 5e). While it is possible that altered function of antigen-presenting cells, which also express Ido, contributed to the T cell effects we observed in mouse GIST, Ido protein was detected predominantly within the actual tumor cells (Fig. 3a).

A role for Etv4 or other *ETS* family transcription factors in *Ido* transcriptional regulation has not been demonstrated. *ETS* family transcription factors are oncogenic in Ewing's sarcoma,

prostate cancer, and melanoma, and have recently been demonstrated to be a lineage survival factor that cooperates with KIT in GIST tumorigenesis.[42] We found that Etv4 was rapidly reduced by imatinib, disrupting its binding to the *Ido* promoter (Fig. 4g). Additionally, imatinib was unable to decrease IDO protein in a resistant GIST cell line (Fig. 4a). This link between oncogenic KIT signaling and the immunosuppressive enzyme IDO suggests that acquired resistance to imatinib, which occurs most frequently due to a secondary *KIT* mutation, may restore intratumoral IDO. Consistent with this hypothesis, we observed that the $CD8^+$ T cell to T reg ratio in human GISTs with acquired resistance to imatinib was significantly lower than in sensitive tumors (Fig. 5c) and resistance was associated with increased *IDO* expression when compared to sensitive tumors (Supplementary Fig. 7). Tumor progression has been associated with IDO recovery in other cancers.[43–45] Thus, molecular and immune resistance in GIST appear to be intertwined.

Although targeted agents are effective, they are not curative, at least for solid tumors. We combined imatinib with CTLA-4 blockade, a well-established immunotherapeutic approach that synergizes with other systemic agents.[46–49] Recently, CTLA-4 blockade proved to be the first treatment to prolong survival in patients with advanced melanoma.[50] That CTLA-4 blockade synergizes with imatinib in mouse GIST demonstrates the potential of combining molecular and immune therapy in human GIST. Our data raise the possibility of treating human melanoma with combined CTLA-4 blockade and either imatinib for *KIT*-mutant tumors[51] or PLX4032 for V600E *BRAF*-mutant tumors.[52,53]

In conclusion, our findings reveal a striking role of T cells in the anti-tumor effects of targeted therapy. Furthermore, oncogenic signaling in GIST is responsible for tumor cell IDO expression, implicating the re-emergence of local immunosuppression as a potential consequence of acquired resistance to targeted therapy. Combined molecular and immune therapy may improve outcomes in human GIST and other cancers that are treated with targeted agents.

MATERIALS AND METHODS

Animals and treatments

We purchased C57Bl/6J (B6), *Rag1*$^{-/-}$, and μMT$^{-/-}$ (*Ighm*^{tm1Cgn}) mice from the Jackson Laboratory and used *Kit*$^{V558\Delta/+}$ mice on a B6 background at 4–8 weeks of age.[10] We used age-matched mice in all experiments. Tumors clustered in weight and size in age-matched GIST mice (data not shown). We dissolved imatinib (Novartis Pharmaceuticals) in sterile endotoxin-free water (HyClone) and injected 1.12 mg i.p. twice daily based on an established dose of 45 mg kg^{-1} or an equivalent volume of sterile water as vehicle control.[11] Greater than 95% depletion of $CD4^+$, $CD8^+$, or $NK1.1^+$ cells was achieved by i.p. injection of 400 μg CD4-specific antibody (clone GK1.5), 250 μg CD8-specific antibody (clone 2.43), or 300 μg NK1.1-specific antibody (clone PK136) on days –3, –2, –1, and 5 with respect to the start of imatinib. We maintained depletion through weekly injections of equivalent amounts of antibody. We obtained antibodies from the Monoclonal Antibody Core Facility, Sloan-Kettering Institute. We prepared and administered 1-MT (Sigma Aldrich) twice daily by oral gavage at 400 mg kg^{-1} as previously described.[54] Methocel/Tween was administered as 1-MT control. We administered L-kynurenine, 3-hydroxyanthranilic acid, and 3-

hydroxykynurenine (Sigma) i.p. as a mixture at 75 mg kg^{-1} per day.[55] We used CTLA-4 blocking antibodies (BioXCell) for induction by injecting 200 μg clone 9H10 i.p. on day 3, 100 ug clone 9H10 i.p. on days 6, 9, and 12, followed by 100 μg of clone 9D9 every 3 d thereafter for long term studies. Animals were maintained in a specific-pathogen free facility at Sloan-Kettering Institute and procedures were approved by the Institutional Animal Care and Use Committee.

Cell Isolation

We obtained single cell suspensions of tumors and DLNs as described in Supplementary Methods. $CD8^+$ T cells were purified with CD8-specific immunomagnetic beads by passing the cells through 2 consecutive positive selection columns (Miltenyi Biotec). Purity was routinely greater than 95% by flow cytometry and cell viability was greater than 97% by trypan blue exclusion. We collected fresh blood and tumor samples from 36 individual patients undergoing elective surgery at Memorial Hospital. Informed consent was obtained according to an Institutional Review Board approved protocol. Blood was drawn at the time of surgery and peripheral blood mononuclear cells were isolated by density centrifugation over Ficoll-Paque Plus (GE Healthcare). We processed tumor tissue immediately following removal from the patient and prepared single-cell suspensions.

Flow Cytometry

We performed flow cytometry on a FACSAria (BD Biosciences) and analyzed data using FlowJo software (Tree Star). Mouse Fc receptors were blocked with 1 μg FcγRIII/II-specific antibody (2.4G2; Monoclonal Antibody Core Facility, Sloan-Kettering Institute) per 10^6 cells. Antibody clones are listed in the Supplementary Methods. We performed intracellular staining for IDO as previously described.[56] We defined T regs as $CD4^+FoxP3^+$.

In vitro assays

GIST-T1 cells have been described previously.[22] GIST-T1R cells were generated by chronic, intermittent culture with imatinib, which resulted in the acquisition of an exon 13 mutation at KIT V654A. We obtained rapamycin from Sigma and treated cells at 50 ng ml^{-1}. We performed ELISPOT for IFN-γ using a kit (BD Biosciences). Briefly, 10^5 T cell-depleted splenocytes were pulsed with a lysate of 10^4 CD117-specific immunomagnetic bead isolated tumor cells (Miltenyi Biotec) for 2 h at 37 °C and plated with 10^5 purified $CD8^+$ T cells for a final volume of 200 μL per well. Plates were incubated for 20 h at 37 °C and developed according to manufacturer's instructions. Spots were counted with an automated ELISPOT reader system and KS 4.3 software (Carl Zeiss).

Microarray, RT-PCR, ChIP analysis, and western blotting

We performed microarray analysis, chromatin immunoprecipitation (ChIP), and western blotting as described in Supplementary Methods. Briefly, chromatin complexes were immunoprecipitated with Etv4 IgG or control IgG. ChIP enriched DNA was subjected to PCR for *Ido* detection. For RT-PCR, we extracted total RNA, reverse transcribed, and amplified cDNA with PCR TaqMan probes for mouse *IL-1*β, *IL-6, TNF*-α, *IL-17, IL-10, TGF*-β, *IFN*-γ, *Ido*, *Etv4*, and *Gapdh* (Applied Biosystems).

Immunohistochemistry

We performed immunohistochemistry and immunofluorescence as detailed in Supplementary Methods.

Imaging

We imaged mice on an R4 microPET (Concorde Microsystems, Knoxville, TN) and analyzed data as previously described.[57] Manually drawn regions-of-interest (ROIs) were used to determine the mean and maximum %ID (decay corrected to the time of injection) in tumors using ASIPro VM™ computer software (Concorde Microsystems). MRI imaging of tumors was performed as previously described.[58] Volumetric analysis was performed using ImageJ software (National Institutes of Health).

Statistics

We performed data analysis using statistical software (Prism 5.0; GraphPad Software, Inc.). Comparisons between two groups were performed using unpaired and paired two-tailed student's *t* test as applicable. Multiple group comparisons were performed using two-way ANOVA using Bonferroni post-test for comparison of individual groups. $P < 0.05$ was considered significant.

Supplementary Material

Refer to Web version on PubMed Central for supplementary material.

ACKNOWLEDGMENTS

We thank members of the Genomics, Tissue Procurement, Monoclonal Antibody, Molecular Cytology, and Animal Imaging core facilities and the Laboratory of Comparative Pathology of Sloan-Kettering Institute. We acknowledge Humilidad F. Gallardo, Yanyun Li, Bushra Zaidi, Teresa Rasalan, Ramon Chua, the Research Animal Resource Center, members of the laboratories of Bhuvanesh Singh and Martin Weiser, and Russell Holmes for technical assistance and logistical support. We are grateful to Gabrielle Rizzuto, Daniel Hirschhorn-Cymerman, David Schaer, Francesca Avogadri, and Taha Merghoub for helpful discussions. We thank Mithat Gonen PhD for statistical assistance. This work was supported by R01 CA102613, the Geoffrey Beene Cancer Research Center, Mr. JHL Pit and Mrs. Pit-van Karnebeek and the Dutch GIST Foundation, GIST Cancer Research Fund, and Swim Across America (R.P.D.); the Society for University Surgeons Ethicon Research Fellowship Award (V.P.B.); R01 CA102774, R01 HL55748, P50 CA140146, LifeRaft Group, and Starr Cancer Consortium (P.B.). Technical services provided by the Animal Imaging Core Facility were supported by the Small-Animal Imaging Research Program (SAIRP) grant R24 CA83084 and P30 CA08748; Molecular Cytology Core Facility by Cancer Center Support Grant NCI P30-CA008748.

REFERENCES

1. Rubin BP, Heinrich MC, Corless CL. Gastrointestinal stromal tumour. Lancet. 2007; 369:1731–1741. [PubMed: 17512858]
2. Hirota S, et al. Gain-of-function mutations of c-kit in human gastrointestinal stromal tumors. Science. 1998; 279:577–580. [PubMed: 9438854]
3. Heinrich MC, et al. PDGFRA activating mutations in gastrointestinal stromal tumors. Science. 2003; 299:708–710. [PubMed: 12522257]
4. Demetri GD, et al. Efficacy and safety of imatinib mesylate in advanced gastrointestinal stromal tumors. N Engl J Med. 2002; 347:472–480. [PubMed: 12181401]

5. Blanke CD, et al. Phase III randomized, intergroup trial assessing imatinib mesylate at two dose levels in patients with unresectable or metastatic gastrointestinal stromal tumors expressing the kit receptor tyrosine kinase: S0033. J Clin Oncol. 2008; 26:626–632. [PubMed: 18235122]

6. Cameron S, et al. Immune cells in primary gastrointestinal stromal tumors. Eur J Gastroenterol Hepatol. 2008; 20:327–334. [PubMed: 18334877]

7. van Dongen M, et al. Anti-inflammatory M2 type macrophages characterize metastasized and tyrosine kinase inhibitor-treated gastrointestinal stromal tumors. Int J Cancer. 2010; 127:899–909. [PubMed: 20013807]

8. Ménard C, et al. Natural killer cell IFN-gamma levels predict long-term survival with imatinib mesylate therapy in gastrointestinal stromal tumor-bearing patients. Cancer Res. 2009; 69:3563–3569. [PubMed: 19351841]

9. Borg C, et al. Novel mode of action of c-kit tyrosine kinase inhibitors leading to NK cell-dependent antitumor effects. J Clin Invest. 2004; 114:379–388. [PubMed: 15286804]

10. Sommer G, et al. Gastrointestinal stromal tumors in a mouse model by targeted mutation of the Kit receptor tyrosine kinase. Proc Natl Acad Sci USA. 2003; 100:6706–6711. [PubMed: 12754375]

11. Rossi F, et al. Oncogenic Kit signaling and therapeutic intervention in a mouse model of gastrointestinal stromal tumor. Proc Natl Acad Sci USA. 2006; 103:12843–12848. [PubMed: 16908864]

12. Zou W. Regulatory T cells, tumour immunity and immunotherapy. Nat Rev Immunol. 2006; 6:295–307. [PubMed: 16557261]

13. Sato E, et al. Intraepithelial CD8+ tumor-infiltrating lymphocytes and a high CD8+/regulatory T cell ratio are associated with favorable prognosis in ovarian cancer. Proc Natl Acad Sci U S A. 2005; 102:18538–18543. [PubMed: 16344461]

14. Quezada SA, Peggs KS, Curran MA, Allison JP. CTLA4 blockade and GM-CSF combination immunotherapy alters the intratumor balance of effector and regulatory T cells. J Clin Invest. 2006; 116:1935–1945. [PubMed: 16778987]

15. Hirschhorn-Cymerman D, et al. OX40 engagement and chemotherapy combination provides potent antitumor immunity with concomitant regulatory T cell apoptosis. J Exp Med. 2009; 206:1103–1116. [PubMed: 19414558]

16. Fallarino F, et al. Modulation of tryptophan catabolism by regulatory T cells. Nat Immunol. 2003; 4:1206–1212. [PubMed: 14578884]

17. Sharma MD, et al. Plasmacytoid dendritic cells from mouse tumor-draining lymph nodes directly activate mature Tregs via indoleamine 2,3-dioxygenase. J Clin Invest. 2007; 117:2570–2582. [PubMed: 17710230]

18. Munn DH, Mellor AL. Indoleamine 2,3-dioxygenase and tumor-induced tolerance. J Clin Invest. 2007; 117:1147–1154. [PubMed: 17476344]

19. Curti A, et al. Modulation of tryptophan catabolism by human leukemic cells results in the conversion of CD25− into CD25+ T regulatory cells. Blood. 2007; 109:2871–2877. [PubMed: 17164341]

20. Baban B, et al. IDO activates regulatory T cells and blocks their conversion into Th17- like T cells. J Immunol. 2009; 183:2475–2483. [PubMed: 19635913]

21. Brenk M, et al. Tryptophan deprivation induces inhibitory receptors ILT3 and ILT4 on dendritic cells favoring the induction of human CD4+CD25+ Foxp3+ T regulatory cells. J Immunol. 2009; 183:145–154. [PubMed: 19535644]

22. Taguchi T, et al. Conventional and molecular cytogenetic characterization of a new human cell line, GIST-T1, established from gastrointestinal stromal tumor. Lab Invest. 2002; 82:663–665. [PubMed: 12004007]

23. Heinrich MC, et al. Primary and secondary kinase genotypes correlate with the biological and clinical activity of sunitinib in imatinib-resistant gastrointestinal stromal tumor. J Clin Oncol. 2008; 26:5352–5359. [PubMed: 18955458]

24. Mellor AL, Munn DH. IDO expression by dendritic cells: tolerance and tryptophan catabolism. Nat Rev Immunol. 2004; 4:762–774. [PubMed: 15459668]

25. Parmar S, et al. Differential regulation of the p70 S6 kinase pathway by interferon alpha (IFNalpha) and imatinib mesylate (STI571) in chronic myelogenous leukemia cells. Blood. 2005; 106:2436–2443. [PubMed: 15790787]
26. Kaur S, et al. Regulatory effects of mammalian target of rapamycin-activated pathways in type I and II interferon signaling. J Biol Chem. 2007; 282:1757–1768. [PubMed: 17114181]
27. Kroczynska B, et al. Interferon-dependent engagement of eukaryotic initiation factor 4B via S6 kinase (S6K)- and ribosomal protein S6K-mediated signals. Mol Cell Biol. 2009; 29:2865–2875. [PubMed: 19289497]
28. Kaur S, et al. Role of the Akt pathway in mRNA translation of interferon-stimulated genes. Proc Natl Acad Sci U S A. 2008; 105:4808–4813. [PubMed: 18339807]
29. Peggs KS, Quezada SA, Allison JP. Cell intrinsic mechanisms of T-cell inhibition and application to cancer therapy. Immunol Rev. 2008; 224:141–165. [PubMed: 18759925]
30. Katz JB, Muller AJ, Prendergast GC. Indoleamine 2,3-dioxygenase in T-cell tolerance and tumoral immune escape. Immunol Rev. 2008; 222:206–221. [PubMed: 18364004]
31. Pedicord VA, Montalvo W, Leiner IM, Allison JP. Single dose of anti-CTLA-4 enhances CD8+ T-cell memory formation, function, and maintenance. Proc Natl Acad Sci U S A. 2011; 108:266–271. [PubMed: 21173239]
32. Klein S, McCormick F, Levitzki A. Killing time for cancer cells. Nat Rev Cancer. 2005; 5:573–580. [PubMed: 15965492]
33. Seggewiss R, et al. Imatinib inhibits T-cell receptor-mediated T-cell proliferation and activation in a dose-dependent manner. Blood. 2005; 105:2473–2479. [PubMed: 15572591]
34. Lee KC, et al. Lck is a key target of imatinib and dasatinib in T-cell activation. Leukemia. 2010; 24:896–900. [PubMed: 20147973]
35. Perez D, et al. Cancer testis antigen expression in gastrointestinal stromal tumors: new markers for early recurrence. Int J Cancer. 2008; 123:1551–1555. [PubMed: 18646188]
36. Zitvogel L, Apetoh L, Ghiringhelli F, Kroemer G. Immunological aspects of cancer chemotherapy. Nat Rev Immunol. 2008; 8:59–73. [PubMed: 18097448]
37. Larmonier N, et al. Imatinib mesylate inhibits CD4+ CD25+ regulatory T cell activity and enhances active immunotherapy against BCR-ABL– tumors. J Immunol. 2008; 181:6955–6963. [PubMed: 18981115]
38. Cohen AD, et al. Agonist anti-GITR monoclonal antibody induces melanoma tumor immunity in mice by altering regulatory T cell stability and intra-tumor accumulation. PLoS One. 2010; 5:e10436. [PubMed: 20454651]
39. Muller AJ, et al. Immunotherapeutic suppression of indoleamine 2,3-dioxygenase and tumor growth with ethyl pyruvate. Cancer Res. 2010; 70:1845–1853. [PubMed: 20160032]
40. Grohmann U, et al. Reverse signaling through GITR ligand enables dexamethasone to activate IDO in allergy. Nat Med. 2007; 13:579–586. [PubMed: 17417651]
41. Uyttenhove C, et al. Evidence for a tumoral immune resistance mechanism based on tryptophan degradation by indoleamine 2,3-dioxygenase. Nat Med. 2003; 9:1269–1274. [PubMed: 14502282]
42. Chi P, et al. ETV1 is a lineage survival factor that cooperates with KIT in gastrointestinal stromal tumours. Nature. 2010; 467:849–853. [PubMed: 20927104]
43. Okamoto A, et al. Indoleamine 2,3-dioxygenase serves as a marker of poor prognosis in gene expression profiles of serous ovarian cancer cells. Clin Cancer Res. 2005; 11:6030–6039. [PubMed: 16115948]
44. Brandacher G, et al. Prognostic value of indoleamine 2,3-dioxygenase expression in colorectal cancer: effect on tumor-infiltrating T cells. Clin Cancer Res. 2006; 12:1144–1151. [PubMed: 16489067]
45. Takao M, et al. Increased synthesis of indoleamine-2,3-dioxygenase protein is positively associated with impaired survival in patients with serous-type, but not with other types of, ovarian cancer. Oncol Rep. 2007; 17:1333–1339. [PubMed: 17487387]
46. Mokyr M, Kalinichenko T, Gorelik L, Bluestone J. Realization of the therapeutic potential of CTLA-4 blockade in low-dose chemotherapy-treated tumor-bearing mice. Cancer Res. 1998; 58:5301. [PubMed: 9850053]

47. van Elsas A, Hurwitz AA, Allison JP. Combination immunotherapy of B16 melanoma using anti-cytotoxic T lymphocyte-associated antigen 4 (CTLA-4) and granulocyte/macrophage colony-stimulating factor (GM-CSF)-producing vaccines induces rejection of subcutaneous and metastatic tumors accompanied by autoimmune depigmentation. J Exp Med. 1999; 190:355–366. [PubMed: 10430624]

48. Hurwitz AA, et al. Combination immunotherapy of primary prostate cancer in a transgenic mouse model using CTLA-4 blockade. Cancer Res. 2000; 60:2444–2448. [PubMed: 10811122]

49. Demaria S, et al. Immune-mediated inhibition of metastases after treatment with local radiation and CTLA-4 blockade in a mouse model of breast cancer. Clin Cancer Res. 2005; 11:728–734. [PubMed: 15701862]

50. Hodi FS, et al. Improved survival with ipilimumab in patients with metastatic melanoma. N Engl J Med. 2010; 363:711–723. [PubMed: 20525992]

51. Curtin JA, Busam K, Pinkel D, Bastian BC. Somatic activation of KIT in distinct subtypes of melanoma. J Clin Oncol. 2006; 24:4340–4346. [PubMed: 16908931]

52. Flaherty KT, et al. Inhibition of mutated, activated BRAF in metastatic melanoma. N Engl J Med. 2010; 363:809–819. [PubMed: 20818844]

53. Bollag G, et al. Clinical efficacy of a RAF inhibitor needs broad target blockade in BRAF-mutant melanoma. Nature. 2010

54. Hou D-Y, et al. Inhibition of indoleamine 2,3-dioxygenase in dendritic cells by stereoisomers of 1-methyl-tryptophan correlates with antitumor responses. Cancer Res. 2007; 67:792–801. [PubMed: 17234791]

55. Jasperson LK, et al. Inducing the tryptophan catabolic pathway, indoleamine 2,3-dioxygenase (IDO), for suppression of graft-versus-host disease (GVHD) lethality. Blood. 2009; 114:5062–5070. [PubMed: 19828695]

56. Lee HJ, et al. Rosmarinic acid inhibits indoleamine 2,3-dioxygenase expression in murine dendritic cells. Biochem Pharmacol. 2007; 73:1412–1421. [PubMed: 17229401]

57. Cho H, et al. Noninvasive multimodality imaging of the tumor microenvironment: registered dynamic magnetic resonance imaging and positron emission tomography studies of a preclinical tumor model of tumor hypoxia. Neoplasia. 2009; 11:247–259. 242p following 259. [PubMed: 19242606]

58. Sotillo R, et al. Mad2 overexpression promotes aneuploidy and tumorigenesis in mice. Cancer Cell. 2007; 11:9–23. [PubMed: 17189715]

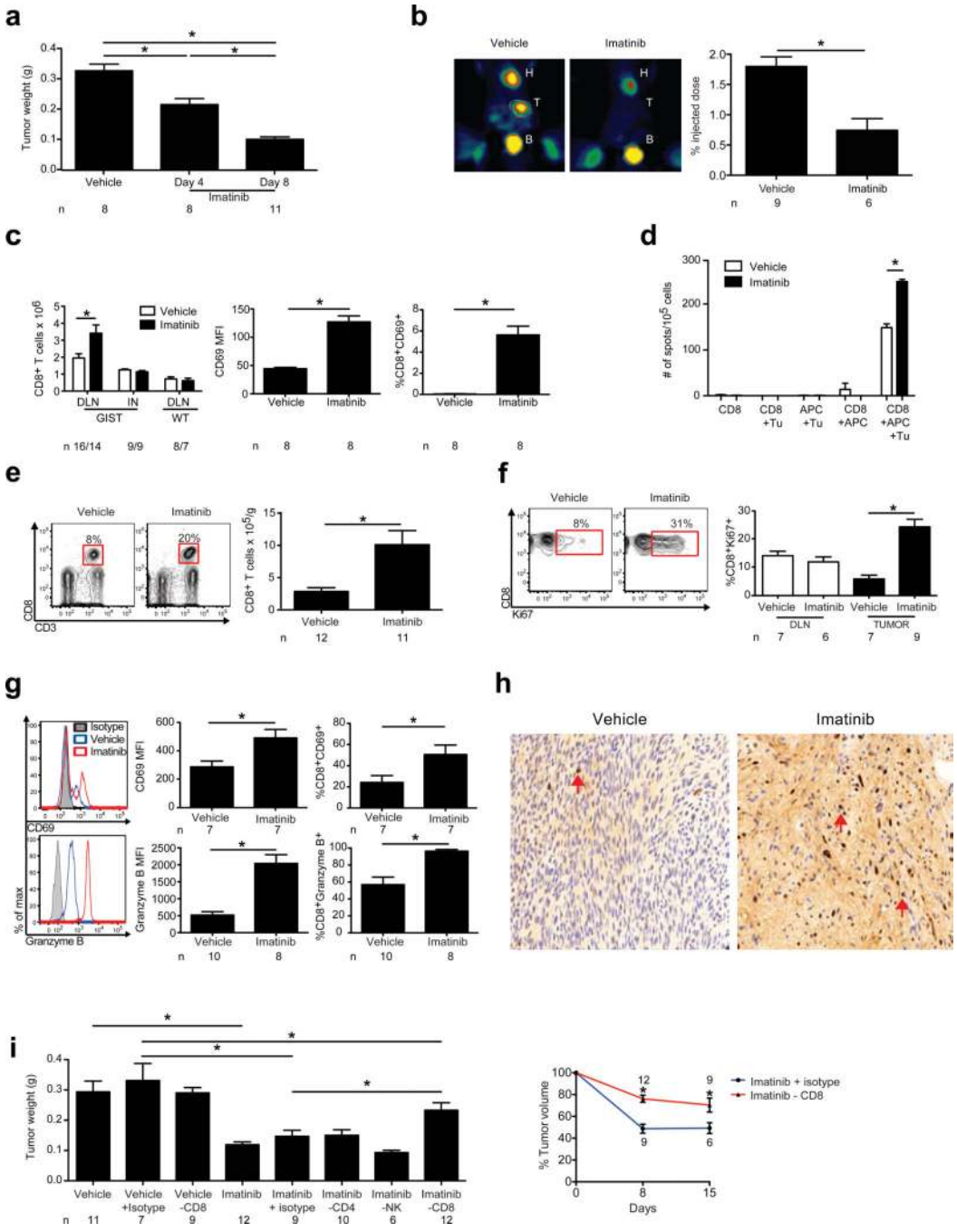

Figure 1. CD8$^+$ T cells contribute to anti-tumor effects of imatinib

GIST and WT mice were treated with vehicle or imatinib and analyzed on days 4 (**a**) or 8 (**a–i**) using flow cytometry, PET, and IHC. (**a**) Tumor weight. (**b**) Tumor uptake of ^{18}FDG by PET. Heart (H), tumor (T), and bladder (B) are indicated. (**c**) Number of CD8$^+$ T cells in the DLN and inguinal node (IN) of GIST mice and mesenteric node of WT mice. Mean fluorescence intensity (MFI), and frequency of CD8$^+$CD69$^+$ T cells in the DLN of GIST mice. (**d**) Purified DLN CD8$^+$ T cells from treated GIST mice were cultured with T cell-depleted splenocytes (APC) and tumor cells (Tu). IFN-γ secretion was determined by

ELISPOT. Average spots per well ± s.e.m. (n = 3 wells) are shown and represent two independent experiments. (**e**) Gating of $CD8^+$ T cells as a frequency of $CD45^+$ lymphocytes (left). Absolute number of intratumoral $CD8^+$ T cells (right). (**f**) Gating and frequency of intratumoral $CD8^+Ki67^+$ T cells. (**g**) Histograms, MFI, and frequency of intratumoral $CD8^+CD69^+$ and $CD8^+$granzyme B^+ T cells. (**h**) Tumors were stained for CD8 (arrows). (**i**) GIST mice were depleted of $CD8^+$ or $CD4^+$ T cells or NK cells during 1 week of imatinib treatment and tumors were weighed (left panel) or during 2 weeks of treatment and measured with magnetic resonance imaging (right panel). Data in (**a–g**, and **i**) represent means ± s.e.m. with $n \geq 6$ per group. $^*P < 0.05$.

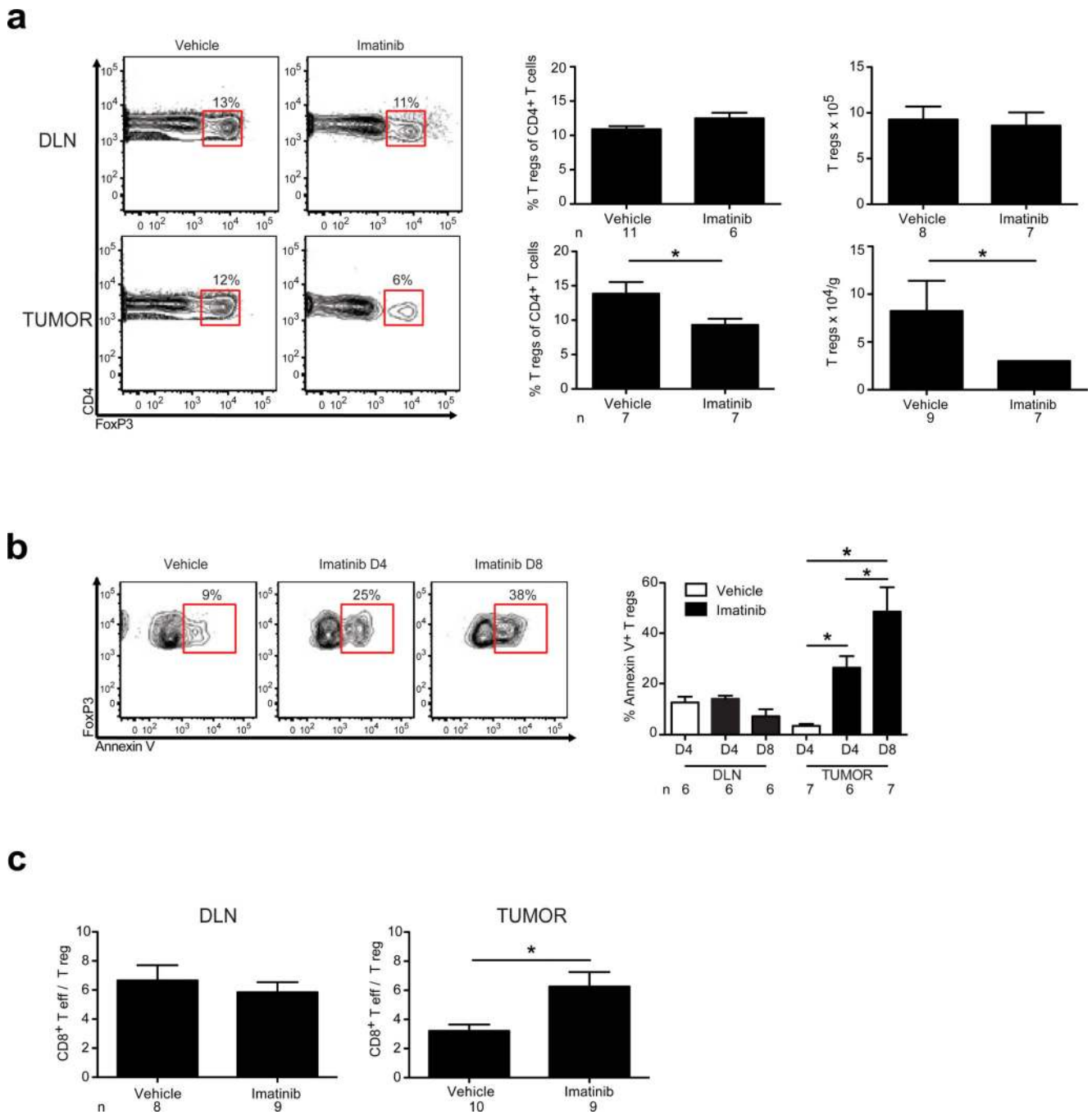

Figure 2. Imatinib induces T reg apoptosis selectively within the tumor

GIST mice were treated with vehicle or imatinib and analyzed by flow cytometry on day 4 (D4) or day 8 (D8). (**a**) Representative gating, frequency, and absolute numbers of DLN and intratumoral T regs on day 8. (**b**) Contour plots demonstrate representative gating of Annexin V expression on intratumoral T regs ($CD4^+FoxP3^+$). Bar graphs represent frequency of Annexin V^+ T regs in the DLN and tumor. Loss of T reg viability was confirmed using propidium iodide staining. (**c**) $CD8^+$ T cell to T reg ratio in the DLN and tumor on day 8. Data represent means ± s.e.m. with $n = 6–11$ per group. $^*P < 0.05$.

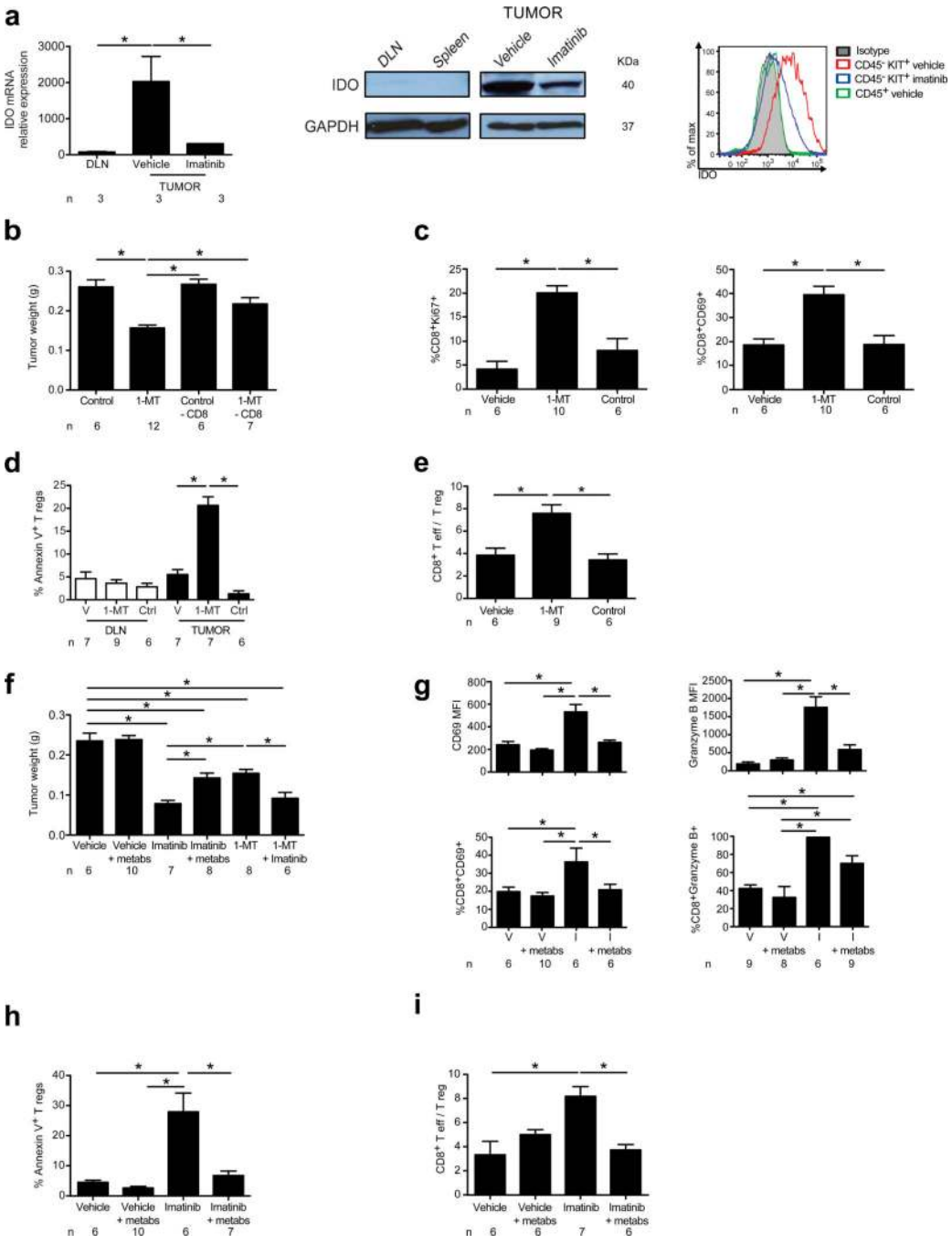

Figure 3. Imatinib alters intratumoral T cells through inhibition of Ido

(**a**) *Ido* mRNA in the DLN and tumor as determined by microarray analysis of vehicle treated GIST mice and the tumor from imatinib treated GIST mice after 7 days (left panel, $n = 3$ per group). Western blot (WB) staining for Ido in the DLN, spleen (center panel, left half), and tumor of vehicle treated GIST mice and tumor of imatinib treated GIST mice (center panel, right half). Intracellular Ido expression in $CD45^+$ intratumoral immune cells and $CD45^-Kit^+$ tumor cells as determined by flow cytometry (right panel). (**b**) Tumor weight of GIST mice treated with 1-MT for 7 d with or without $CD8^+$ T cell depletion. (**c–i**)

GIST mice were treated for 7 d with combinations of 1-MT or control (Ctrl), imatinib (I), or vehicle (V), and tryptophan metabolites (metabs). Tumors and DLNs were analyzed using flow cytometry. (**c**) Frequency of intratumoral $CD8^+Ki67^+$ and $CD8^+CD69^+$ T cells. (**d**) Frequency of intratumoral Annexin V^+ T regs. (**e**) Intratumoral $CD8^+$ T cell to T reg ratio. (**f**) Tumor weight. (**g**) MFI and frequency of intratumoral $CD8^+CD69^+$ and $CD8^+$granzyme B^+ T cells. (**h**) Frequency of intratumoral Annexin V^+ T regs. (**i**) Intratumoral $CD8^+$ T cell to T reg ratio. Data in (**a**) left panel represent means ± s.e.m. and are shown relative to internal controls (housekeeping gene). Data represent means ± s.e.m. with $n = 6–12$ per group. $^*P < 0.05$.

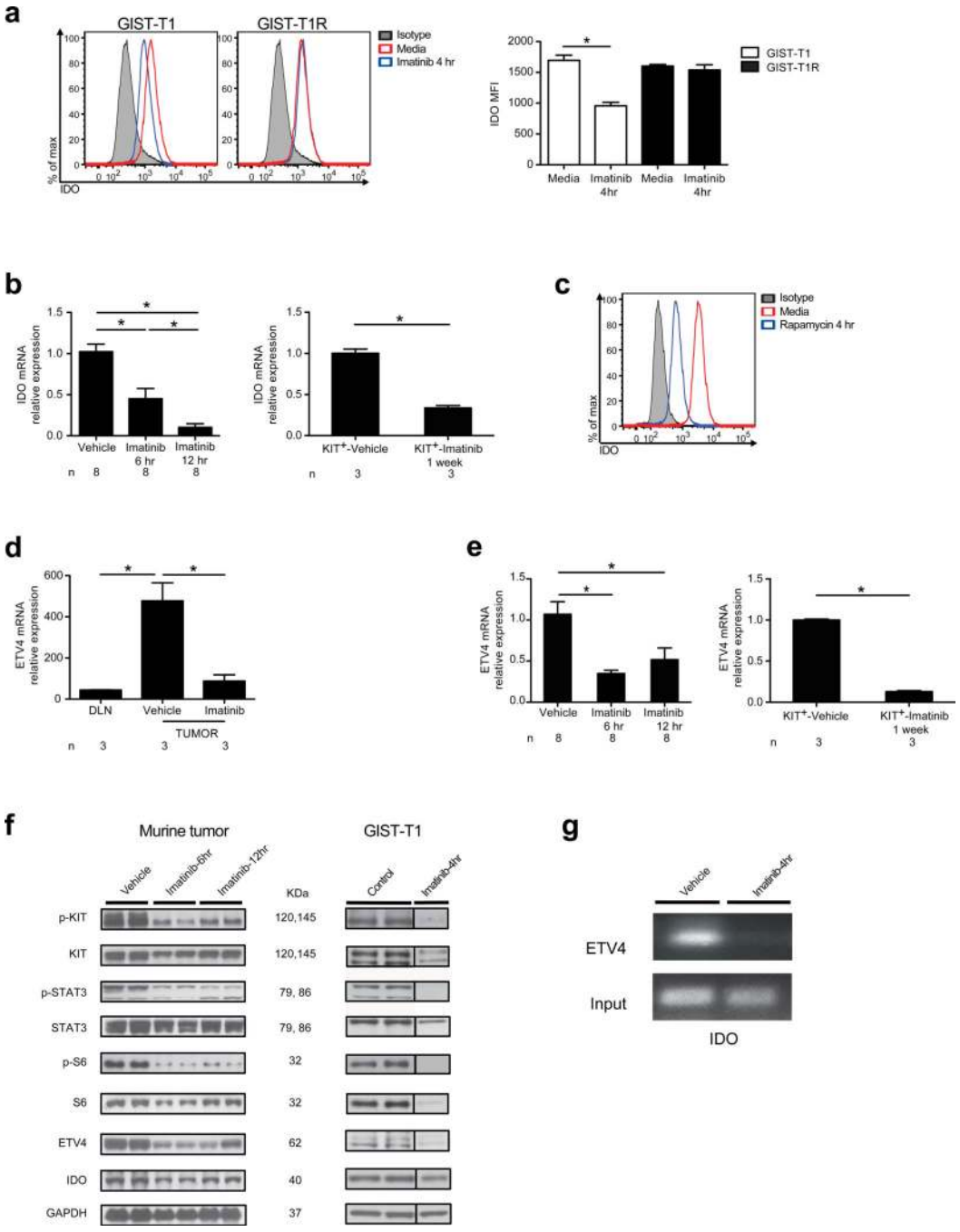

Figure 4. Imatinib reduces IDO expression through inhibition of oncogenic KIT signaling

(**a**) IDO in GIST-T1 and GIST-T1R cells. (**b**) *Ido* mRNA in mouse GIST tumors (left panel, $n = 8$ per group) and sorted Kit$^+$ tumor cells (right panel, $n = 3$ per group shown relative to internal controls) after treatment with vehicle or imatinib. (**c**) Intracellular IDO in GIST-T1 cells after culture in rapamycin. (**d**) *Etv4* mRNA in the DLN and tumor determined by microarray analysis from GIST mice after vehicle or imatinib treatment for 7 d. $n = 3$ per group shown relative to internal controls. (**e**) *Etv4* mRNA in mouse GIST tumors (left panel, $n = 8$ per group) and sorted Kit$^+$ tumor cells (right panel, $n = 3$ per group) after treatment

with vehicle or imatinib. (**f**) WB of KIT, ETV4, and IDO in GIST mice (left panel) and GIST-T1 cells (right panel) after treatment with vehicle, control, or imatinib. Both phosphorylated and non-phosphorylated KIT, STAT3, and S6 are shown as components of oncogenic KIT signaling. IDO in GIST-T1 cells was detected via immunoprecipitation. (**g**) Chromatin immunoprecipitation (ChIP) was performed on GIST mice treated with vehicle or imatinib *in vivo* ($n = 3$ per group). *In vitro* culture experiments were performed with 1 μM imatinib. Data in (**b**) and (**e**) were normalized to internal controls and are shown relative to vehicle treatment. Data represent means ± s.e.m. with n as indicated above, or triplicate wells analyzed individually and representative plots are shown. $^{*}P < 0.05$.

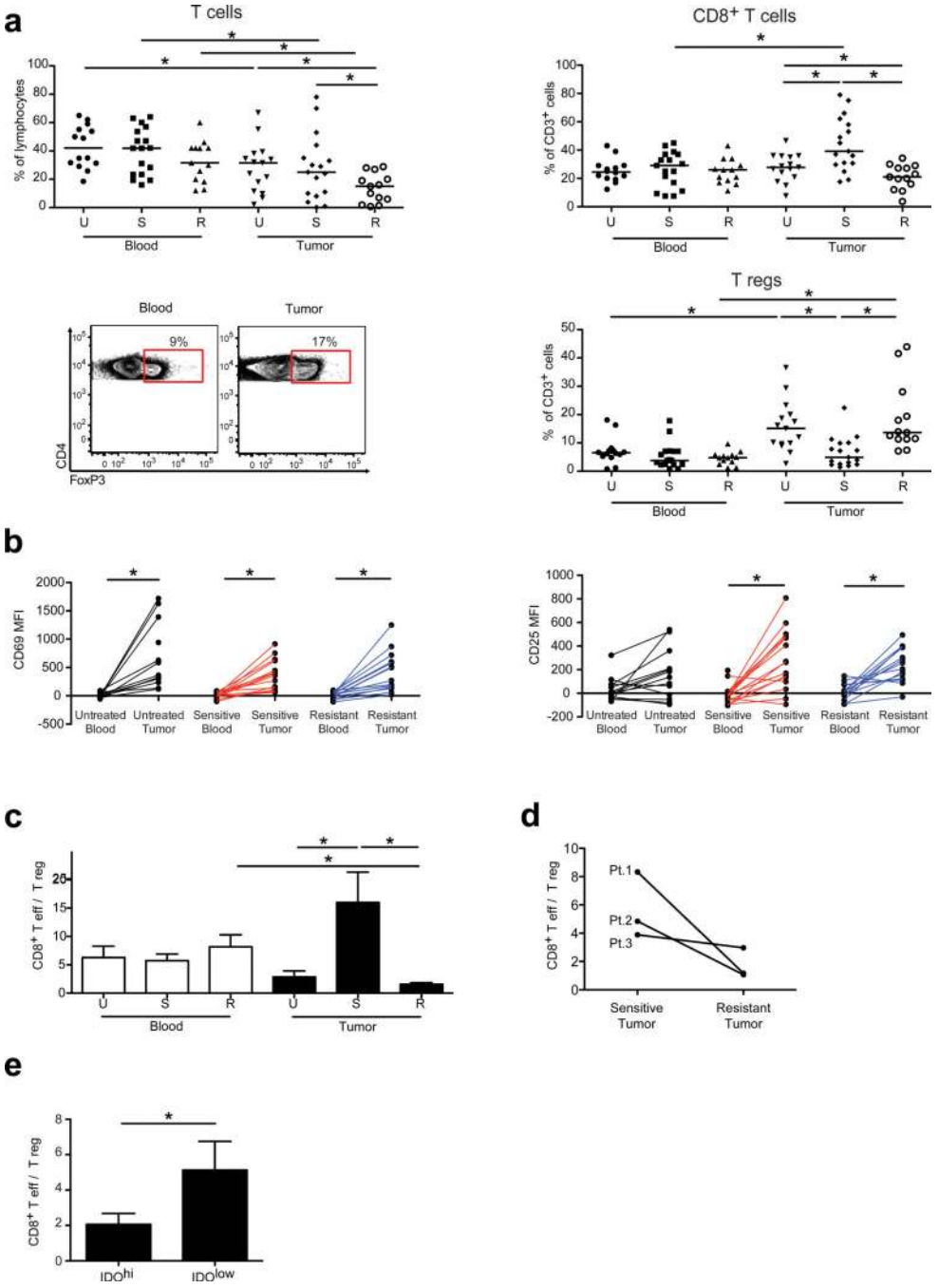

Figure 5. Intratumoral CD8$^+$ T cell to T reg ratio correlates with imatinib sensitivity in human GIST

(**a**) Flow cytometrically determined frequency of CD3$^+$ and CD8$^+$ T cells and T regs in peripheral blood and tumor of untreated (U; n = 15), sensitive (S; n = 17), and resistant (R; n = 13) GIST specimens and representative gating for T regs. (**b**) CD69 and CD25 expression on CD8$^+$ T cells from matched peripheral blood and tumor samples. (**c**) CD8$^+$ T cell to T reg ratio in blood and tumor. (**d**) CD8$^+$ T cell to T reg ratio in 3 patients (Pt.) who underwent synchronous resection of a sensitive and resistant tumor. (**e**) CD8$^+$ T cell to T reg ratio in

tumors expressing low (< 4,000 MFI, $n = 6$) or hi (≥4,000, $n = 7$) IDO protein as determined by flow cytometry. Data in (**c,e**) represent means ± s.e.m. *$P < 0.05$.

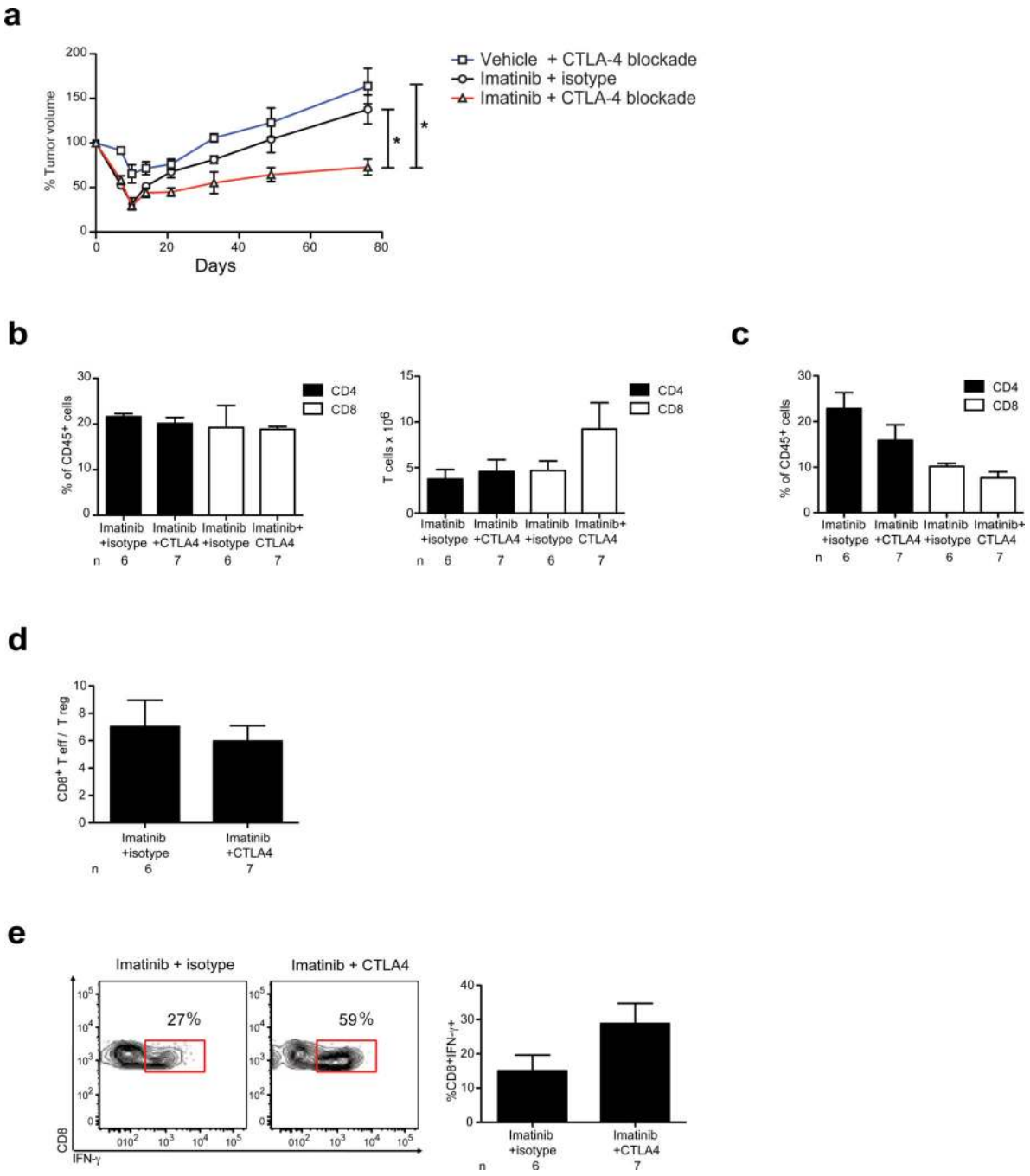

Figure 6. CTLA-4 blockade is synergistic with imatinib

GIST mice were treated with imatinib or vehicle for 7 d with or without induction CTLA-4 blockade or isotype control antibody followed by chronic CTLA-4 blockade. (**a**) Tumor size was monitored using serial MRIs. (**b–e**) Tumors and DLNs of GIST mice were analyzed on days 16–18 to determine (**b**) frequency and absolute number of $CD4^+$ and $CD8^+$ T cells in DLN, (**c**) frequency of intratumoral $CD4^+$ and $CD8^+$ T cells, and (**d**) intratumoral $CD8^+$ T cell to T reg ratio. (**e**) Intratumoral $CD8^+$ T cells were stimulated for 4 h with phorbol 12-myristate 13-acetate and ionomycin followed by intracellular analysis for IFN-γ production;

$P = 0.09$, two-tailed student t-test. Data in (**a**) represent means ± s.e.m. of a composite of two independent experiments each with 3–5 mice per group. Data in (**b–e**) represent means ± s.e.m. with $n = 6–8$ per group. *$P < 0.05$.